JCI insight

Free light chains injure proximal tubule cells through STAT1-HMGB1-TLR axis

Rohit Upadhyay, … , Paul W. Sanders, Vecihi Batuman

JCI Insight. 2020. https://doi.org/10.1172/jci.insight.137191.

Research In-Press Preview Cell biology Nephrology

Graphical abstract

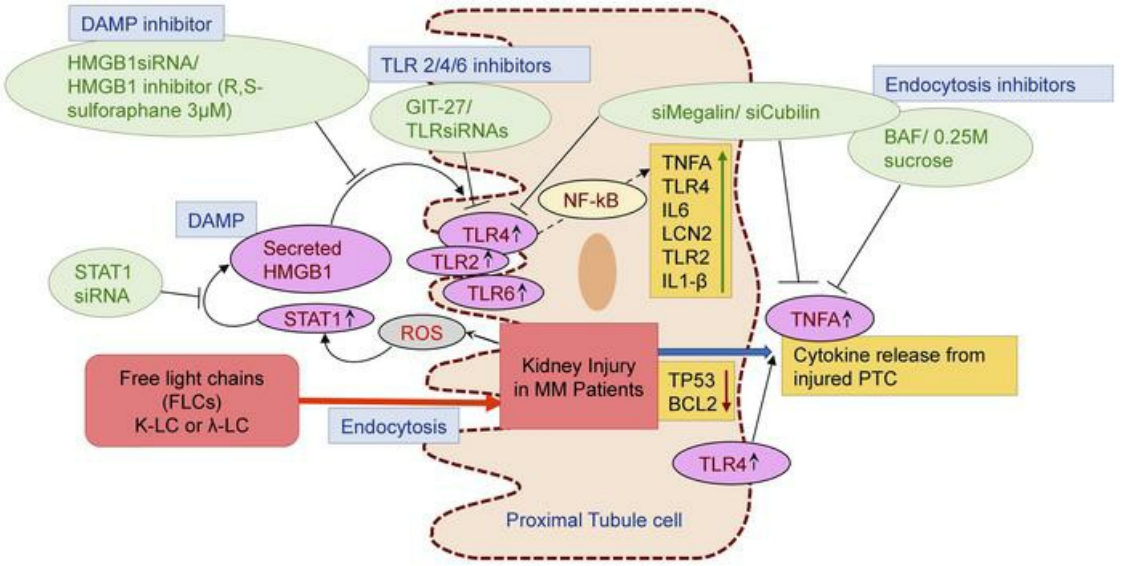

Find the latest version:

https://jci.me/137191/pdf

FREE LIGHT CHAINS INJURE PROXIMAL TUBULE CELLS THROUGH STAT1-HMGB1-TLR AXIS

Rohit Upadhyay[1], Wei-Zhong Ying[2], Zannatul Nasrin[1], Hana Safah[1], Edgar A. Jaimes[3], Wenguang Feng[2], Paul W. Sanders[2,4,#], Vecihi Batuman[1,5*,#]

[1]John W. Deming Department of Medicine, Tulane University School of Medicine, New Orleans, LA.

[2]University of Alabama at Birmingham, Birmingham, AL.

[3]Department of Medicine, Renal Service, Memorial Sloan Kettering Cancer Center, NY

[4]Department of Veterans Affairs Medical Center, Birmingham, AL

[5]Department of Veterans Affairs Southeast Louisiana Veterans Health Care System, New Orleans, LA

***Corresponding Author:**

Vecihi Batuman, MD

Division of Nephrology and Hypertension,

John W. Deming Department of Medicine,

Tulane University School of Medicine, SL-45, 1430 Tulane Avenue, New Orleans, LA 70112, USA.

Tel: +1-504-988-5346, Fax: 504-988-1909

E-mail: vbatuma@tulane.edu

[#]**Authorship Note:** Paul W. Sanders and Vecihi Batuman contributed equally to this work.

Conflict of interest statement: EAJ is chief medical officer and share holder of Goldilocks Therapeutics, Inc. All other authors have declared no conflict of interest.

Abstract

Free light chains (FLCs) induce inflammatory pathways in proximal tubule cells (PTCs). The role of toll-like receptors (TLR) in these responses is unknown. Here we present findings on the role of TLRs in FLC-induced PTC injury.

We exposed human kidney PTC cultures to κ and λ FLCs, and used cell supernatants and pellets for ELISA and gene expression studies. We also analyzed tissues from *Stat1*$^{-/-}$ and littermate control mice treated with daily intraperitoneal injections of a κ-FLC for 10 days.

FLCs increased the expression of TLRs 2, 4, 6 via HMGB1, a damage-associated molecular pattern. Countering TLRs 2, 4, and 6 through GIT-27 or specific TLR-siRNAs reduced downstream cytokine responses. Blocking HMGB1 through siRNA or pharmacologic inhibition, or via STAT1 inhibition reduced FLC-induced TLRs 2, 4, and 6 expression. Blocking endocytosis of FLCs through silencing of megalin/cubilin, with bafilomycin-A1, or hypertonic sucrose attenuated FLC-induced cytokine responses in PTCs. Immunohistochemistry showed decreased TLR 4 and 6 expression in kidney sections from *Stat1*$^{-/-}$ mice compared to their littermate controls.

PTCs exposed to FLCs released HMGB1, which induced TLRs 2, 4, 6 expression and downstream inflammation. Blocking FLCs' endocytosis, *Stat1* knock-down, HMGB1 inhibition, and TLR knock-down each rescued PTCs from FLC-induced injury.

Keywords: TLRs, Free light chains, Kidney injury, HMGB1, STAT1, Endocytosis

Introduction

Multiple myeloma (MM) is a cancer of mature B cells or plasma cells. In healthy state, plasma cells produce a slight excess of immunoglobulin free light chains (FLCs), both kappa (κ), and lambda (λ), that are efficiently endocytosed and catabolized by the kidney proximal tubule cells (PTC), and only minute amounts of FLC proteins normally appear in the urine (1). In MM, FLCs are produced in excessive quantities and overwhelm the endocytic capacity of PTCs (2). Overloading endocytic pathways elicits cell stress responses resulting in activation of inflammatory pathways and cell injury leading to a worse prognosis in patients with MM (2-4). Nephrotoxic effects of FLCs include a cascade of inflammatory effects, such as, generation of reactive oxygen species, activation of mitogen-activated protein kinases (MAPK) and nuclear factor kappa-light-chain-enhancer of activated *B* cells (NF-κB), followed by transcription and secretion of inflammatory and profibrotic cytokines, apoptosis and epithelial-mesenchymal transition of PTCs (5-11).

In the initial stages, the kidney effects may appear as subtle proximal tubule function alterations including Fanconi syndrome (7-9). These changes often progress to more severe tubulo-interstitial kidney disease leading to either acute kidney injury or chronic tubulointerstitial disease with or without cast nephropathy (1, 7, 8, 12-14). In many cases, the progression of kidney disease is indolent and often recognized late with the consequence of delayed therapy further compromising prognosis.

Although a clearer picture of the inflammatory events surrounding FLC nephrotoxicity has emerged from the recent studies, there are still unanswered questions. For example, an overview of the inflammatory phenomena noted in PTCs exposed to FLCs and in animal models (6, 9) raises the possibility that innate immunity may play a role, but this has not been investigated in the setting of FLC cytotoxicity. In this current work we present our findings on the

role of toll-like receptors (TLRs), tools of innate immunity, in the inflammatory effects of myeloma FLCs on human PTCs.

Results

FLCs caused injury to PTCs and decreased proliferation rate in a dose-dependent manner. Expression of kidney injury marker LCN2 (Lipocalin 2); also known as Neutrophil Gelatinase-Associated Lipocalin (NGAL), was increased in PTCs (HK2 cells) exposed to FLCs (T-κ1 or T-λ1) for 24 hrs but not in control cells (Figure 1A). Cell proliferation of PTCs decreased significantly upon exposure to high concentrations (200-400 μM) of FLCs (6): T-κ (3) and T-λ (3) for 24 hrs; [Supplementary Figure 1]. The 25 μM concentration of FLCs selected for present study corresponds to the levels expected in MM patients with modest FLC proteinuria (4).

LCN2 gene expression in RPTECs was upregulated when incubated with T-κ1 and T-λ1 FLCs (25 μM each for 24 hrs; N=5), in comparison to untreated (No LC) or BSA (160 μM) treated cells (Figure 1B).

FLCs induced significant upregulation of kidney injury biomarkers. Screening of candidate genes (*TLR2*, *TLR3*, *TLR4*, *TLR6*, *TLR9*, *HMGB1*, *MYD88*, *TICAM1*, *IL6*, *IL18*, *IL1B*, *IL2*, *TNFA*, *TGFB*, *BCL2*, *TP53*, *HAVCR1*, *ABCB1* and *LCN2*) was performed by qPCR to associate their expressions with injury in PTCs exposed with 6 different FLCs (N = 5 in each group) for 24hrs. A heat-map of gene expressions was constructed with hierarchical clustering of the data (Figure 2). We found that *TNFA, TLR4, MYD88, IL6, LCN2, CUBN, TLR2* and *IL-1B* were upregulated in PTCs exposed to six different FLCs, while *TP53* and *BCL2* were downregulated.

TNFA appeared prominently among the top candidate gene markers in PTCs exposed to FLCs. To validate this observation, we checked TNFA protein levels in PTCs after exposure to varying concentrations (25-400 μM) of T-κ1- and T-λ1 FLCs for 24hrs or 48hrs. TNFA levels increased in PTCs in a dose- and time-dependent manner after exposure to either FLC isotype ($P<0.05$; Figure 3A-B). We used this assay as an indicator of FLCs toxicity in PTCs throughout this study.

FLCs upregulated the expression of TLRs 2, 4, 6 and their downstream adaptor protein molecules MYD88 and TRIF. After exposure to six different FLCs (three T-κ and three T-λ), the mRNA and protein levels of TLR2, TLR4 and TLR6 were significantly upregulated in PTCs ($P<0.05$; Figure 4 A-D, G-I). Specifically, TLR4 was significantly upregulated by six different FLCs. Both MyD88- and TRIF-dependent pathways were activated as mRNA expression of both adaptor proteins were significantly upregulated (Figure 4 E-F); however, MYD88 was more significantly upregulated with most of the FLCs used in these studies (five of the six FLCs).

Proximal tubule cells released HMGB1 into the medium when exposed to the FLCs. Activation of TLR is mediated by unique ligands, such as, pathogen-associated molecular patterns (PAMPs), or damage-associated molecular patterns (DAMPs). HMGB1 is one of the key DAMPs that is known to activate TLR4 signaling. Therefore, we assayed HMGB1 levels by ELISA in PTCs exposed to six different FLCs for 24-hr. Remarkably, six different FLCs (3 A-κ and 3 A-λ FLCs) induced significant HMGB1 release into the medium from PTCs in comparison with cells treated with vehicle or bovine serum albumin (BSA; $N = 8$; $P < 0.05$; Figure 5A). This finding suggested that PTCs injured by FLCs exposure release HMGB1 to activate TLRs on the proximal tubule cells.

Lu et al. showed that the JAK/STAT1 pathway participates integrally in the release of HMGB1 by promoting the hyperacetylation of multiple amino acid residues that include those within the two nuclear localization sites on HMGB1 (15). This post-translational modification permits the movement of HMGB1 out of the nucleus and subsequent release into the extracellular space. Because this pathway is activated by FLCs in the proximal tubule, we hypothesized that the STAT1 pathway mediated the FLC-induced release of HMGB1. Consistent with prior results (5), the siRNA that targeted STAT1 effectively reduced STAT1 protein (Figure 5B). The reduction in STAT1 decreased the FLC-mediated HMGB1 release (Figure 5C). These data supported the role of the STAT1 pathway in this process.

FLCs induced TLR expression in vivo. Analysis of changes in mRNA expression in kidney cortex of *Stat1*$^{+/+}$ mice treated with FLCs for 10 days showed increased expression of TLR2, 4 and 6 compared with control mice. These increases were mitigated in *Stat1*$^{-/-}$ mice, although the changes in TLR4 did not differ between the *Stat1*$^{+/+}$ and *Stat1*$^{-/-}$ groups. We then performed IHC studies and attempted to stain for TLRs 2, 4, and 6 in kidney sections from these same *Stat1*$^{+/+}$ and *Stat1*$^{-/-}$ mice treated with FLCs (5). While staining for TLR2 was unsuccessful, staining for TLR4 and 6 was strongly (score= 3+) or moderately strongly (score= 2+) positive in the *Stat1*$^{+/+}$ mice predominantly in the proximal tubules, but was negative (score= 0) or only trace positive (score= 1+) in *Stat1*$^{-/-}$ mice kidneys (Figure 5 D-E). This experiment confirms that TLR activation is involved in FLC-mediated inflammation in the kidney, and also that STAT1 plays a pivotal role in the activation of inflammatory pathways in the FLC-exposed kidney.

FLCs activated TLRs through HMGB1. To validate our hypothesis that induced HMGB1 release activates TLRs, we modulated HMGB1 expression in PTCs either with introduction of extracellular HMGB1 (100ng/ml) for over-expression or with HMGB1 siRNA for inhibition of HMGB1 expression in the presence or absence of FLCs.

HMGB1 ELISA results confirmed that extracellular HMGB1 (100ng/ml) was detectable after treatment with a T-κ and a T-λ FLC (similar to A- FLCs), while HMGB1 siRNA inhibited HMGB1 release into the media of FLC-exposed PTCs (Figure 6A). Furthermore, we assessed the TLR2, 4, 6 expression in PTCs with or without FLC treatment and while modulating medium HMGB1 concentration. Addition of HMGB1 increased expression of TLR 2 (2.56 fold change; P=0.0012), TLR 4 (1.88 fold change; P=0.03), and TLR 6 (1.60 fold change; P=0.08) proteins. Further, HMGB1knock-down (by siRNA or by R,S Sulforaphane) inhibited the expected increase in TLRs 2, 4, 6 that occurred with FLC treatment, which suggests HMGB1 as a regulator of TLRs 2, 4, 6 activation in PTCs (Figure 6B-F).

Inhibition of TLR expression reduced FLC-induced TNFA release. To evaluate whether the FLC-induced release of TNFA by PTCs was mediated by TLR signaling, we treated PTCs with TLR2,4,6 signaling inhibitor GIT27. Addition of the inhibitor prevented secretion of TNFA (Figure 7A-C) indicating that TLR activation is involved in FLC-induced cytokine release. Through dose response analysis we found that GIT27 at 150 μM prevented the secretion of TNFA from the RPTECs (Figure 7D). Additionally, we used pooled sets of siRNAs to knock down *TLR2, 4* and *6* genes individually and in combination. We found that *TLR2/4/6*-siRNAs also reduced FLC-induced TNFA expression in PTCs again pointing to the role of TLR activation in production of TNFA (Figure 7E).

Blocking endocytosis of FLCs inhibited TNFA release and expression of TLR4 and TNFA. We used hypertonic sucrose solution (0.25M), which inhibits receptor-mediated endocytosis by interfering with clathrin-coated pit formation, and bafilomycin A1 (1μM), a V-ATPase inhibitor, to block endocytosis of FLCs into PTCs (12). Both of these maneuvers to inhibit endocytosis had a protective effect on PTCs exposed to FLCs, as they both significantly decreased TNFA release from PTCs in response to FLC exposure ($P<0.05$, Figure 8A). Furthermore, we silenced megalin and cubilin genes using specific pooled siRNAs as another maneuver to inhibit endocytosis (4) and again noted a marked decrease in FLCs-induced expressions of *TNFA* and *TLR4* genes (Figure 8 B, C).

DISCUSSION

Up to 50% of newly diagnosed patients with multiple myeloma (MM) have kidney involvement (16), which can lead to a rapid decline in organ function and organ failure (17-19) and is associated with worse prognosis in MM (20). It has been estimated that there will be 32,110 new cases of myeloma and an estimated 12,960 people may die (2.1 % of all cancer deaths) of this disease in year 2019 in United States (SEER Cancer Stat Facts: Myeloma. National Cancer Institute. Bethesda, MD, (Percent survival in 5 years – 2009-2015, 52.2%) https://seer.cancer.gov/statfacts/html/mulmy.html). Early diagnosis and intervention remain keys for preventing irreversible renal injury in patients with MM.

In the early stages of MM, FLC nephrotoxicity may present with proximal tubule functional abnormalities. Overproduction of monoclonal FLCs is a major factor in the pathophysiology of myeloma kidney, although a direct correlation between quantity and nephrotoxicity does not exist, indicating variable toxicity among FLC species. Our previous work demonstrated that inflammatory pathways triggered by the endocytosis of FLCs in the proximal tubule cells play a significant role in the pathophysiology of FLC-associated kidney injury (KI) (21). Studies based on in vitro exposure of kidney cells to FLCs from myeloma patients provided considerable insight into the pathophysiology of kidney disease in MM (2-4, 10, 11, 22-24). Li *et al.*, (4) demonstrated that FLC endocytosis is predominantly mediated by the megalin-cubilin tandem endocytic receptor and blocking light chain endocytosis helps in preventing its nephrotoxic effects on human kidney PTCs. We also have published studies that showed endocytosis of FLC in RPTECs leads to activation of NF-κB and inflammatory pathways, along with epithelial-mesenchymal transition (4, 9, 13, 25). Although inflammatory pathways responsible for these lesions have been identified, the precise mechanisms intiating these responses are still not clear. Specifically, the role of innate immunity mediated by TLRs has not been explored. TLRs are a family of evolutionarily conserved trans-membrane pattern/damage-recognition receptors

that can generate a cascade of signaling events that lead to the production of myriad cytokines and effector molecules (26). TLRs are currently being explored as therapy targets, since interference with their signaling pathways can limit tumor formation. Enhancing their activity could provide an adjuvant therapy to standard treatments (27). Our current knowledge of the function of TLRs has gone beyond the main role as triggers of innate and adaptive immune responses (28-30). TLRs play a major role in the pathogenesis of hypoxia/ischemia-induced and other types of AKI (31-34). In the present study, we have aimed to explore the pathophysiologic role of TLRs in FLC-induced injury in kidney proximal tubule cells. Our data showed that TLRs may be major mediators of human FLC-induced PTC injury.

The present studies also demonstrated that FLCs promoted a STAT1-dependent release of HMGB1. High Mobility Group (HMG) proteins comprise a large superfamily that has three subfamilies: HMGA, HMGB and HMGN. HMGs have a common carboxyl terminus, but each has a unique functional motif that confers distinct cellular functions (35). These nuclear proteins are involved in the regulation of chromatin dynamics. However, HMGB1 in particular is released into the extracellular fluid in inflammatory states (36). Unlike the other two HMGB family members, HMGB1 promotes additional biological functions by serving as a ligand particularly for TLR2 and TLR4 to effect the elaboration of cytokines and chemokines (37). As a prototypical alarmin, which is an endogenously derived danger signal molecule (36), HMGB1 was produced by PTCs exposed to FLCs and directly involved in the inflammatory responses mediated through the TLRs.

Proximal tubulopathy and “myeloma kidney,” which is now known as cast nephropathy, comprise the two most common types of kidney involvement in patients with MM. Proximal tubulopathy may be associated with tubule dysfunction including proximal tubular acidosis (type 2) clinically. Cast nephropathy is predominantly a chronic tubulointerstitial disease that spares the glomeruli and is characterized by interstitial fibrosis and tubule atrophy as well as tubule

casts formed by binding of FLCs to Tamm-Horsfall protein (1, 7, 8, 38). FLCs are responsible for the majority of kidney lesions seen in myeloma. The occurrence of casts in myeloma kidney is highly variable, may be extensive in some cases, especially in acute cast nephropathy and exceedingly sparse in others. In either case, there is a prominent feature of tubulointerstitial injury with extensive fibrosis and tubule atrophy. The present study elaborates a mechanism whereby some FLCs facilitate fibrosis and tubule atrophy by causing cell injury in the absence of obstructive casts. These studies confirm the pivotal role of STAT1 in initiating these inflammatory responses through the release of HMGB1, a major ligand responsible for the activation of TLRs, from injured proximal tubule cells. The findings further suggest new pathways for intervention in limiting chronic kidney disease in MM.

Materials and Method:

Subject Population: Twelve different FLCs, six κ and six λ, were isolated and purified from MM patients from Tulane hospital, Memorial Sloan Kettering Cancer Center, and the University of Alabama at Birmingham. The study protocol was approved by the Human Research Committee and all protected health information was deidentified. All twelve patients had mild to moderate kidney disease with light-chain proteinuria but without significant albuminuria, comprising a group of patients predominantly with tubulointerstitial disease.

Urine Collection and FLC Isolation: FLCs were purified from the urine of patients who had multiple myeloma, light chain proteinuria, and clinical evidence of significant renal damage that was presumed to be cast nephropathy, using standard methods described previously (3, 12, 21, 23). Briefly, urine samples were precipitated with ammonium sulfate (Millipore Sigma; Cat#A-5132) (55 to 90% saturation-determined empirically), extensively dialyzed against distilled water and lyophilized. The crude FLCs were purified by dissolving in buffer at pH 6.0 followed by chromatography on CM-Sephadex C-50 (Millipore Sigma; Cat#C-50120) column; bound FLCs were eluted with 0.6 M of NaCl, re-dialyzed and lyophilized. The purity and identity of FLCs were confirmed by SDS-PAGE and Western blotting. FLCs, isolated from the urine, purified and stored in lyophilized form were used for the experiments. The FLCs from the UAB laboratory were labeled A-κ2, A-κ3, A-κ6, A-λ2, A-λ3, and A-λ5. The FLCs from Tulane were labeled as T-κ1, T-κ2, T-κ3, T-λ1, T-λ2, and T-λ3. All specimens were determined to be endotoxin free. FLCs were pathogen and endotoxin free.

Cell cultures: We used human kidney proximal tubule cells (PTCs), cell lines: RPTECs (ATCC®; Cat#CRL-4031™) and HK2 (ATCC®; Cat#CRL-2190™)], to evaluate the effect of κ and λ light chains. We cultured and prepared cells for experiments as previously described (4, 11, 21, 23, 39). Briefly, cells were grown (passage<10) on Cell-bind® surface flasks/ 6 well plates (Corning, Tewksbury, MA) and incubated at 37°C with 5% CO2. RPTECs were cultured

in DMEM/F12 medium (ATCC®, Manassas, VA; Cat#30-2006) with REGM SingleQuote kit Supplements & growth factors (Lonza, Walkersville, MD; Cat#CC-4127) and HK2 cells were cultured in keratinocyte serum-free medium (K-SFM; Cat#10744019) (Gibco, Invitrogen, Thermo Fisher Scientific) supplemented with recombinant human epidermal growth factor (5 ng/ml) and bovine pituitary extract (50 µg/ml). Media was exchanged at 48-hour intervals. The cells were exposed to both κ and λ FLCs at varying doses and time intervals. Cell supernatant was collected for ELISA and cell pellet was used for gene expression studies. Based on our dose-time screening data we used a minimum concentration of FLCs (25 µM) for a minimum exposure time of 24-hours.

Animal and Tissue Preparation: Colonies of *Stat1* knockout mice (termed *Stat1*$^{-/-}$ mice) and littermate controls (termed *Stat*$^{+/+}$ mice) were developed and confirmed by PCR-based genotyping and maintained in a gnotobiotic facility, as described previously (5). All animal studies were conducted using animal biosafety level 3 laboratory and Sealsafe cages with HEPA filters, and personnel wore personal protective equipment. *Stat1*$^{-/-}$ mice grew normally and were phenotypically normal under these conditions. Eight-week-old male *Stat1*$^{+/+}$ and *Stat1*$^{-/-}$ mice (n = 8-10/group) were intraperitoneally injected daily with either phosphate-buffered saline (PBS) alone (Invitrogen, Carlsbad, CA) as Vehicle or with the κ2 FLC at a lower dose (termed κ2-d1= 0.033 mg/g BW) or higher dose (termed κ2-d2= 0.165 mg/g BW) of κ2 FLC in PBS. The experiments were concluded on day 10 and the left kidney was harvested for histology and immunohistochemistry (5).

Cell proliferation assay: To check the effect of FLCs on proliferation of PTCs, CellTiter 96® AQueous One Solution Cell Proliferation Assay (MTS) (Promega Madison, WI; Cat#G3580) was used. Cells were seeded in 96-well plates ($1.0X10^4$ cells/well) and exposed to FLCs for indicated time periods followed by the MTS assay. MTS assays were performed by adding a small amount (20µl) of the CellTiter 96® AQueous One Solution Reagent directly to culture

wells, incubating for 2 hours and then recording absorbance at 490nm with Bio-tek Synergy™ HT Multi-Detection Microplate Reader (Biotek®, Winooski, VT, USA).

Immunocytochemistry: Immunofluorescence microscopy was performed using 4% paraformaldehyde (PFA) fixed HK2 cells. Cells were permeabilized with triton-X100 (0.1%) and 2% BSA in PBS. Cells were blocked in normal goat serum (Cell signaling technology, Boston MA; Cat#5425S), 0.1% Triton X-100 (PBST) for 1 hour. Slides were incubated in LCN2 primary antibody (Abcam; Cat#Ab63929; dilution 1:100) that were diluted in blocking buffer overnight at 4°C. Cells were washed in PBST (3 times). Goat anti-Rabbit IgG (H+L) Superclonal™ Secondary Antibody, Alexa Fluor 555 (Thermo Fisher Scientific; Pittsburgh, PA, USA; Cat#A27039) was used at concentration of 1.0 µg/mL (1:1000) in phosphate buffered saline containing 0.2 % BSA for 1 hour at room temperature. Samples were then washed in PBST, rinsed in phosphate buffer, and No. 1.5 cover slips were mounted with UltraCruz® Aqueous Mounting Medium with DAPI (Santa Cruz Biotechnology; Cat#sc-24941). Images were captured on an upright Nikon Eclips 80i fluorescent microscope (NIKON, Tokyo, Japan) at x40 magnification).

Molecular inhibitors/mimics and siRNA transfections: To knock down the expression of a specific gene we used commercially available siRNAs or known molecular inhibitors. *Stat1* siRNA (Cat#SR304620, OriGene Technology), HMGB1 siRNA (Cat#AM16708; Ambion, Thermo Fisher Scientific), pooled siRNA (3 to 5 target specific) for TLR2 (Cat#sc-40256, Santa Cruz Biotechnology Inc.), TLR4 (Cat#sc-40260, Santa Cruz Biotechnology Inc., TLR 6(Cat#sc-40264, Santa Cruz Biotechnology Inc.), Megalin siRNA (Cat#sc-40103; Santa Cruz Biotechnology Inc.), and Cubilin siRNA (Cat#sc-40100, Santa Cruz Biotechnology Inc.) were used for corresponding gene knock-down experiments. As a control for transfection, control siRNA-A (Cat#sc-37007, Santa Cruz Biotechnology Inc.) was used, which consists of a scrambled sequence.

Molecular inhibitors used to inhibit HMGB1 were (R,S Sulforaphane; 3 μM; Enzo Life Sciences, Inc. Farmingdale, NY, USA; Cat#ALX-350-232-M025),TLR2,4,6 (GIT27, 150 μM, TOCRIS, Bio-Techne Corporation Minneapolis, MN, USA; Cat#3270) and endocytosis inhibitor (bafilomycin, 1μM, Sigma-Aldrich, St. Louis, MO, USA; Cat#B1793). As a molecular mimic, extracellular HMGB1 (100ng/ml, Sigma-Aldrich, St. Louis, MO, USA; Cat#SRP6265) was used to modulate HMGB1 expression in cultured RPTECs in presence or absence of FLCs.

Enzyme-linked immunosorbent assay (ELISA): The levels of TNFA and HMGB1 in the cell culture medium were determined with ELISA assay kits (Thermo Fisher Scientific; Pittsburgh, PA, USA; Cat#BMS223-4 and Tecan Inc., NC, USA; Cat#ST51011 respectively) according to the manufacturer's instructions.

Real Time quantitative polymerase chain reaction (qPCR): Total RNA was isolated from cultured proximal tubule cells using the RNeasy Plus Mini Kit (Qiagen, Germantown, MD; Cat#74136). Total RNA (0.2-1μg) of purified RNA was used to prepare cDNA through high capacity RNA to c-DNA kit (Applied Biosystems, Foster City, CA; Cat#4368814). Candidate gene expressions were estimated using the fluorescent dye SYBR green methodology and CFX96 Touch™ Real-Time PCR machine (BioRad, Hercules, California). Bio-informatically validated primer sets (QuantiTect Primer Assays, Qiagen or IDT, Germany) were purchased for use in SYBR Green-based real-time RT-PCR. Real-time fluorescence from SYBR Green^{R} (Applied Biosystems, Foster City, CA) was measured by the Bio-Rad CFX Manager 3.1 System Software. Gene expression was normalized to the endogenous controls (beta-actin or *GAPDH*) and comparative CT values were estimated. Relative gene expression was calculated through $2^{-(\Delta\Delta CT)}$ method and expressed in arbitrary units [a.u] relative to paired controls. Heat-map of gene expressions was generated by using "Heatmapper" web-server (40). Hierarchical clustering was done as Average Linkage and Euclidian method was used for distance measurement between clusters.

To analyze the expression of TLRs in mice, total RNA was extracted from kidney cortex with TRIzol (Invitrogen, Carlsbad, CA; Cat#15596018), treated with DNAase I (Invitrogen; Cat#18068015) to remove carry-over genomic DNA and then purified with use of an RNA purification kit (Ambion, Carlsbad, CA). The DNA-free RNA was reverse-transcribed to cDNA with SuperScript IV (Invitrogen; Cat#18090200). Candidate gene expressions were estimated using the fluorescent dye SYBR green methodology and Roche LightCycler480 Real-Time PCR machine (Roche, Indianapolis, IN). Primer sets (IDT, Coralville, IA) were purchased for use in SYBR Green-based real-time RT-PCR. Real-time fluorescence from SYBR Green^{R} (Applied Biosystems, Foster City, CA) was measured by the LightCycler480 System Software. Gene expression was normalized to the endogenous controls GAPDH and comparative CT values were estimated. Relative gene expression was calculated through $2^{-(\Delta\Delta CT)}$ method and expressed in fold-change relative to the vehicle control group.

Western Blotting: Protein was isolated from cells and quantified through Pierce™ BCA Protein Assay Kit (Thermo Fisher Scientific; Pittsburgh, PA, USA; Cat#23225). Immunoblotting was done to detect the expression of proteins with antibodies against TLR2 (Santa Cruz Biotechnology Inc. Dallas, TX, USA; Cat#sc-21759; dilution 1:200), TLR4 (Santa Cruz Biotechnology Inc. Dallas, TX, USA; Cat#sc-293072; dilution 1:200), TLR6 (ProSci Inc.; Poway, CA, USA; Cat#3651; dilution 1:1000)) and β-actin (LI-COR Biotechnology, Lincoln, NE, USA; Cat# 926-42212; dilution 1:1000). Equal amounts of proteins (10-20 µg) were separated through Bolt™ 4-12% Bis-tris gel (Thermo Fisher Scientific; Pittsburgh, PA, USA; Cat#NW04122BOX) electrophoresis and transferred onto nitrocellulose membrane (LI-COR Biotechnology, Lincoln, NE, USA; Cat#926-31092). The membrane was blocked either with PBS, TBS or 5% milk in Tris-buffered saline-Tween (TBST 0.05%) solution based on primary antibody-specific recommendations by the manufacturing company. After overnight incubation with primary antibody blots were incubated with LI-COR secondary antibody (Odyssey IRDye® 680RD;

Cat#926-68070 or 800CW; Cat# 926-32211) for 1-hr. Western blots were visualized by Odyssey® CLx Imaging System (LI-COR Biotechnology, Lincoln, NE, USA) utilizing near-infrared (NIR) fluorescence capture. Western blot image analysis was done using Image Studio™ (LI-COR Biotechnology, Lincoln, NE, USA) software to obtain the integrated intensities. Data analysis was done after normalizing with endogenous control protein (beta-actin or GAPDH).

Immunohistochemistry for Toll-like Receptors: Immunohistochemistry for TLRs 2, 4 and 6 was performed in kidney sections prepared from the same *Stat1*$^{+/+}$ and *Stat1*$^{-/-}$ mice studied by Ying *et. al.,* in recently reported experiments, which demonstrated that the STAT1 served as the key signaling molecule that produced the proinflammatory molecule IL-1ß, as well as the profibrotic agent TGF-β in the proximal tubule epithelium (5). Immunostaining was done following a standard protocol at Tulane pathology core facility. Briefly, slides were dispensed in 150µl reagents in each step. Blocking was performed with 5 minutes incubation in H_2O_2, 10 minutes each with Avidin and Biotin for auxiliary blocking. Retrieval step was performed manually at pH 6.0 with Citrate rodent solution (Biocare Medical; Pacheco, CA, USA; Cat#CB910M) and NxGen Decloaker was used for 15 minutes at 110°C. After rinsing non-specific proteins were blocked for 30 minutes with Rodent Block M (Biocare Medical; Pacheco, CA, USA; Cat#RBM961 G). Slides were rinsed and incubated for 45 minutes with TLR 4 (Santa Cruz Biotechnology Inc. Dallas, TX, USA; Cat#sc-293072; dilution 1:250) and TLR 6 (ProSci Inc.; Poway, CA, USA; Cat#3651; dilution 1:100) primary antibodies. Da Vinci Green (Biocare Medical; Pacheco, CA, USA; Cat#PD900 H) diluent was used for antibody dilutions. Slides were incubated with secondary antibodies for 30 minutes, mouse on mouse HRP (Biocare Medical; Pacheco, CA, USA; Cat#MM620) and rabbit on rodent (Biocare Medical; Pacheco, CA, USA; Cat#RMR 622) secondary antibodies were used for TLR4 and TLR6 staining respectively. Beta-diaminobenzideine (DAB) was incubated for 5 minutes as substrate and CAT-Hematoxylin

(Biocare Medical; Pacheco, CA, USA; Cat#CATHE-M) was used in 1:5 dilution in 1X TBS buffer for counterstaining. Biocare Nemesis (LVMA-LV1.3-0187) automated stainer was used to run all experimental slides under uniform conditions. Stained sections were imaged at x20 magnification using fluorescent microscope (M5000, Thermo Scientific) and representative images were used for scorings.

The staining intensity of the TLR4 and TLR6 as well as the 1:5 CAT Hematoxylin counterstaining as a labeling index (percentage of positive nuclei) was evaluated and scored by a single experienced pathologist, Lorene Yoxtheimer, MD. The paraffin sections were prepared from *Stat1*$^{+/+}$ and *Stat1*$^{-/-}$ mice previously reported by Ying *et. al.,* (5), and the sections were coded such that the pathologist was blinded to the experimental design and the source of the kidney sections. TLR2 staining yielded no staining in the *Stat1*$^{+/+}$ or *Stat1*$^{-/-}$ mice. TLR4 and TLR6 staining were interpretable and the slides were scored as 0 (absence of staining) (negative), and 1+ (weakly positive), 2 + (moderately positive), and 3+ (intense staining) (strongly positive).

Statistical Analysis: Data were analyzed by comparing mean values through either Student's t-test (for comparing 2 groups) or one-way ANOVA (for comparing multiple groups) or two-way ANOVA with Tukey's multiple comparison post-hoc test. P values < 0.05 were assumed significant. Data were expressed as mean ± standard error of mean (S.E.M.). Data were analyzed by using GraphPad Prism software version 8.3.0 (GraphPad software, San Diego, CA, USA). All experiments were performed at least in triplicate.

Study Approval: This study was approved by the Institutional Review Board (IRB) at Tulane Office of Human Research Protection (IRB Reference #: 848169). In addition, the Birmingham VA Institutional Review Board provided annual continuing IRB oversight and approval of this research activity. This study was carried out in strict accordance with the recommendations in

the Guide for the Care and Use of Laboratory Animals of the National Institutes of Health. The Institutional Animal Care and Use Committee at the University of Alabama at Birmingham approved the project.

Author contributions: VB and RU conceived the study and designed experiments. VB and PWS secured funding for the project and helped with manuscript preparation. RU, ZN, W-ZY, and WF designed and performed the experiments and analyzed data. RU, VB, and PWS wrote and edited the manuscript. All authors read the manuscript, provided input and approved the final submission. PWS and VB contributed equally to this work.

Acknowledgement: Supported by Paul Teschan Research Fund (VB), by a Merit Award (1 I01 CX001326) from the United States Department of Veterans Affairs Clinical Sciences R&D (CSRD) Service (PWS) and a National Institutes of Health George M. O'Brien Kidney and Urological Research Centers Program (P30 DK079337) (PWS), and by P30CA008748 (EAJ)

References:

1. Hutchison CA, Batuman V, Behrens J, Bridoux F, Sirac C, Dispenzieri A, et al. The pathogenesis and diagnosis of acute kidney injury in multiple myeloma. *Nat Rev Nephrol.* 2011;8(1):43-51.
2. Batuman V. Proximal tubular injury in myeloma. *Contrib Nephrol.* 2007;153:87-104.
3. Batuman V, Verroust PJ, Navar GL, Kaysen JH, Goda FO, Campbell WC, et al. Myeloma light chains are ligands for cubilin (gp280). *Am J Physiol.* 1998;275(2 Pt 2):F246-54.
4. Li M, Balamuthusamy S, Simon EE, and Batuman V. Silencing megalin and cubilin genes inhibits myeloma light chain endocytosis and ameliorates toxicity in human renal proximal tubule epithelial cells. *Am J Physiol Renal Physiol.* 2008;295(1):F82-90.
5. Ying WZ, Li X, Rangarajan S, Feng W, Curtis LM, and Sanders PW. Immunoglobulin light chains generate proinflammatory and profibrotic kidney injury. *J Clin Invest.* 2019;130:2792-806.
6. Sirac C, Herrera GA, Sanders PW, Batuman V, Bender S, Ayala MV, et al. Animal models of monoclonal immunoglobulin-related renal diseases. *Nat Rev Nephrol.* 2018;14(4):246-64.
7. Doshi M, Lahoti A, Danesh FR, Batuman V, Sanders PW, and American Society of Nephrology Onco-Nephrology F. Paraprotein-Related Kidney Disease: Kidney Injury from Paraproteins-What Determines the Site of Injury? *Clin J Am Soc Nephrol.* 2016;11(12):2288-94.
8. Sanders PW. Mechanisms of light chain injury along the tubular nephron. *J Am Soc Nephrol.* 2012;23(11):1777-81.
9. Batuman V. The pathogenesis of acute kidney impairment in patients with multiple myeloma. *Adv Chronic Kidney Dis.* 2012;19(5):282-6.

10. Khan AM, Li M, Balamuthusamy S, Maderdrut JL, Simon EE, and Batuman V. Myeloma light chain-induced renal injury in mice. *Nephron Exp Nephrol.* 2010;116(2):e32-41.
11. Li M, Hering-Smith KS, Simon EE, and Batuman V. Myeloma light chains induce epithelial-mesenchymal transition in human renal proximal tubule epithelial cells. *Nephrol Dial Transplant.* 2008;23(3):860-70.
12. Batuman V, and Guan S. Receptor-mediated endocytosis of immunoglobulin light chains by renal proximal tubule cells. *Am J Physiol.* 1997;272(4 Pt 2):F521-30.
13. Sanders PW. Light chain-mediated tubulopathies. *Contrib Nephrol.* 2011;169:262-9.
14. Ying WZ, and Sanders PW. Mapping the binding domain of immunoglobulin light chains for Tamm-Horsfall protein. *Am J Pathol.* 2001;158(5):1859-66.
15. Lu B, Antoine DJ, Kwan K, Lundback P, Wahamaa H, Schierbeck H, et al. JAK/STAT1 signaling promotes HMGB1 hyperacetylation and nuclear translocation. *Proc Natl Acad Sci U S A.* 2014;111(8):3068-73.
16. Knudsen LM, Hippe E, Hjorth M, Holmberg E, and Westin J. Renal function in newly diagnosed multiple myeloma--a demographic study of 1353 patients. The Nordic Myeloma Study Group. *Eur J Haematol.* 1994;53(4):207-12.
17. Nasr SH, Valeri AM, Sethi S, Fidler ME, Cornell LD, Gertz MA, et al. Clinicopathologic correlations in multiple myeloma: a case series of 190 patients with kidney biopsies. *Am J Kidney Dis.* 2012;59(6):786-94.
18. Masai R, Wakui H, Togashi M, Maki N, Ohtani H, Komatsuda A, et al. Clinicopathological features and prognosis in immunoglobulin light and heavy chain deposition disease. *Clin Nephrol.* 2009;71(1):9-20.
19. Gertz MA. Managing light chain deposition disease. *Leuk Lymphoma.* 2012;53(2):183-4.
20. Mohan M, Buros A, Mathur P, Gokden N, Singh M, Susanibar S, et al. Clinical characteristics and prognostic factors in multiple myeloma patients with light chain deposition disease. *Am J Hematol.* 2017;92(8):739-45.

21. Sengul S, Zwizinski C, Simon EE, Kapasi A, Singhal PC, and Batuman V. Endocytosis of light chains induces cytokines through activation of NF-kappaB in human proximal tubule cells. *Kidney Int.* 2002;62(6):1977-88.

22. Li M, Maderdrut JL, Lertora JJ, Arimura A, and Batuman V. Renoprotection by pituitary adenylate cyclase-activating polypeptide in multiple myeloma and other kidney diseases. *Regul Pept.* 2008;145(1-3):24-32.

23. Sengul S, Erturk S, Khan AM, and Batuman V. Receptor-associated protein blocks internalization and cytotoxicity of myeloma light chain in cultured human proximal tubular cells. *PLoS One.* 2013;8(7):e70276.

24. Sengul S, Li M, and Batuman V. Myeloma kidney: toward its prevention--with new insights from in vitro and in vivo models of renal injury. *J Nephrol.* 2009;22(1):17-28.

25. Arimura A, Li M, and Batuman V. Treatment of renal failure associated with multiple myeloma and other diseases by PACAP-38. *Ann N Y Acad Sci.* 2006;1070:1-4.

26. El-Achkar TM, and Dagher PC. Renal Toll-like receptors: recent advances and implications for disease. *Nat Clin Pract Nephrol.* 2006;2(10):568-81.

27. Thakur KK, Bolshette NB, Trandafir C, Jamdade VS, Istrate A, Gogoi R, et al. Role of toll-like receptors in multiple myeloma and recent advances. *Exp Hematol.* 2015;43(3):158-67.

28. Abdi J, Garssen J, and Redegeld F. Toll-like receptors in human multiple myeloma: new insight into inflammation-related pathogenesis. *Curr Mol Med.* 2014;14(4):423-31.

29. Abdi J, Mutis T, Garssen J, and Redegeld F. Characterization of the Toll-like Receptor Expression Profile in Human Multiple Myeloma Cells. *PLoS One.* 2013;8(4):e60671.

30. Abdi J, Mutis T, Garssen J, and Redegeld FA. Toll-like receptor (TLR)-1/2 triggering of multiple myeloma cells modulates their adhesion to bone marrow stromal cells and enhances bortezomib-induced apoptosis. *PLoS One.* 2014;9(5):e96608.

31. Amura CR, Renner B, Lyubchenko T, Faubel S, Simonian PL, and Thurman JM. Complement activation and toll-like receptor-2 signaling contribute to cytokine production after renal ischemia/reperfusion. *Mol Immunol.* 2012;52(3-4):249-57.

32. Arumugam TV, Okun E, Tang SC, Thundyil J, Taylor SM, and Woodruff TM. Toll-like receptors in ischemia-reperfusion injury. *Shock.* 2009;32(1):4-16.

33. Khan AM, Li M, Abdulnour-Nakhoul S, Maderdrut JL, Simon EE, and Batuman V. Delayed administration of pituitary adenylate cyclase-activating polypeptide 38 ameliorates renal ischemia/reperfusion injury in mice by modulating Toll-like receptors. *Peptides.* 2012.

34. Li M, Khan AM, Maderdrut JL, Simon EE, and Batuman V. The effect of PACAP38 on MyD88-mediated signal transduction in ischemia-/hypoxia-induced acute kidney injury. *Am J Nephrol.* 2010;32(6):522-32.

35. Hock R, Furusawa T, Ueda T, and Bustin M. HMG chromosomal proteins in development and disease. *Trends Cell Biol.* 2007;17(2):72-9.

36. Diener KR, Al-Dasooqi N, Lousberg EL, and Hayball JD. The multifunctional alarmin HMGB1 with roles in the pathophysiology of sepsis and cancer. *Immunol Cell Biol.* 2013;91(7):443-50.

37. Bianchi ME, and Manfredi AA. High-mobility group box 1 (HMGB1) protein at the crossroads between innate and adaptive immunity. *Immunol Rev.* 2007;220:35-46.

38. Ying WZ, Allen CE, Curtis LM, Aaron KJ, and Sanders PW. Mechanism and prevention of acute kidney injury from cast nephropathy in a rodent model. *J Clin Invest.* 2012;122(5):1777-85.

39. Sengul S, Zwizinski C, and Batuman V. Role of MAPK pathways in light chain-induced cytokine production in human proximal tubule cells. *Am J Physiol Renal Physiol.* 2003;284(6):F1245-54.

40. Babicki S, Arndt D, Marcu A, Liang Y, Grant JR, Maciejewski A, et al. Heatmapper: web-enabled heat mapping for all. *Nucleic Acids Res.* 2016;44(W1):W147-53.

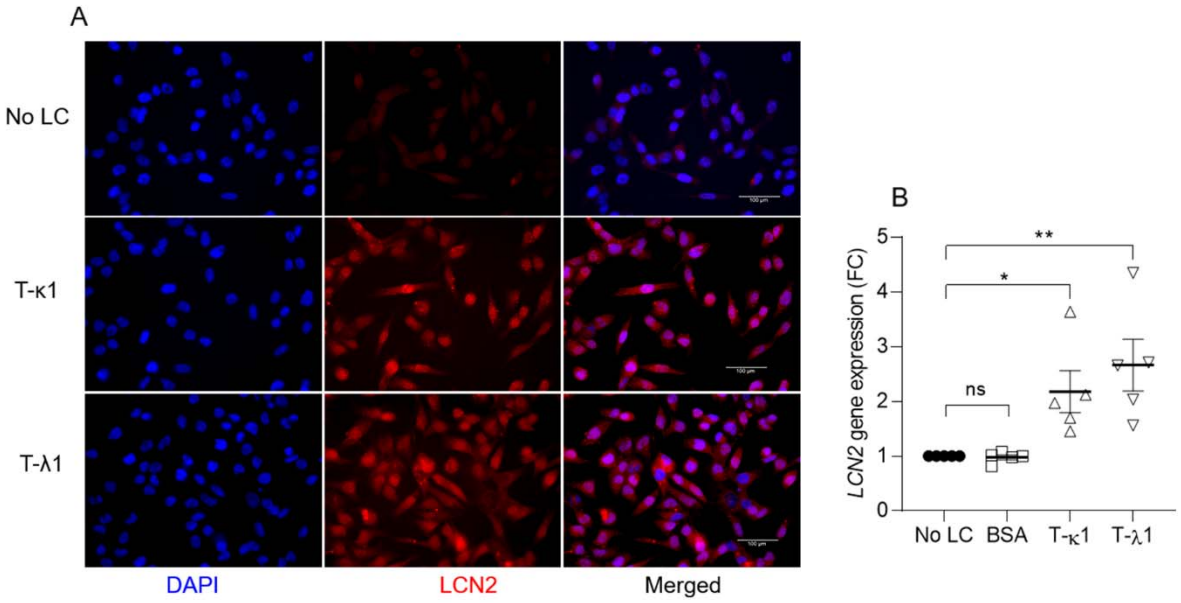

Figure1. A: T-κ1 and T-λ1 FLC exposure (25μM each for 24hrs) to Human proximal tubule cells (PTCs; HK2) caused cellular injury evident by the increased expression of known KI marker LCN2 (DAPI- blue, LCN2- red) in comparison to untreated (No LC) cells; **B:** *LCN2* gene expression significantly increased in RPTECs exposed with T-κ1 and T-λ1 FLCs (25μM each for 24hrs; N=5) in comparison to untreated (No LC) or BSA (160 μM) treated cells. **P*<0.05, ***P*<0.01; (one-way ANOVA followed by Tukey's multiple comparisons test).

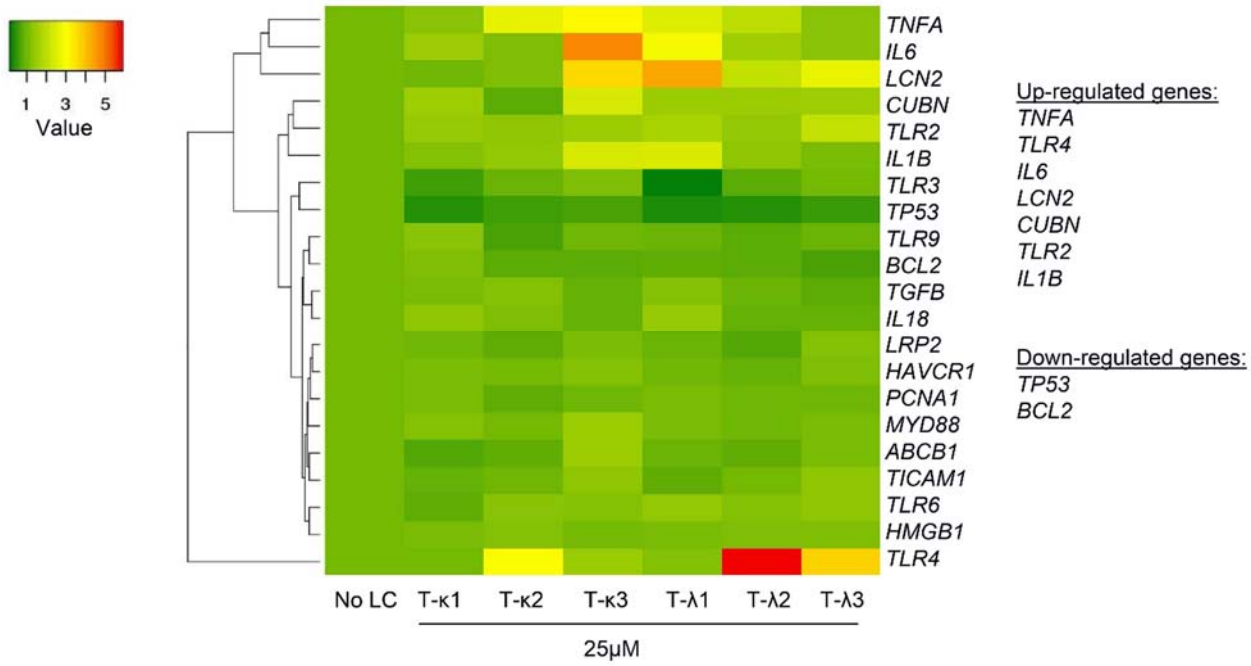

Figure 2. Heat-map of candidate gene expressions with hierarchical clustering in PTCs (RPTECs) exposed with 6 different FLCs (T-κ1, T-κ2, T-κ3, T-λ1, T-λ2, T-λ3; N= 5) for 24 hrs

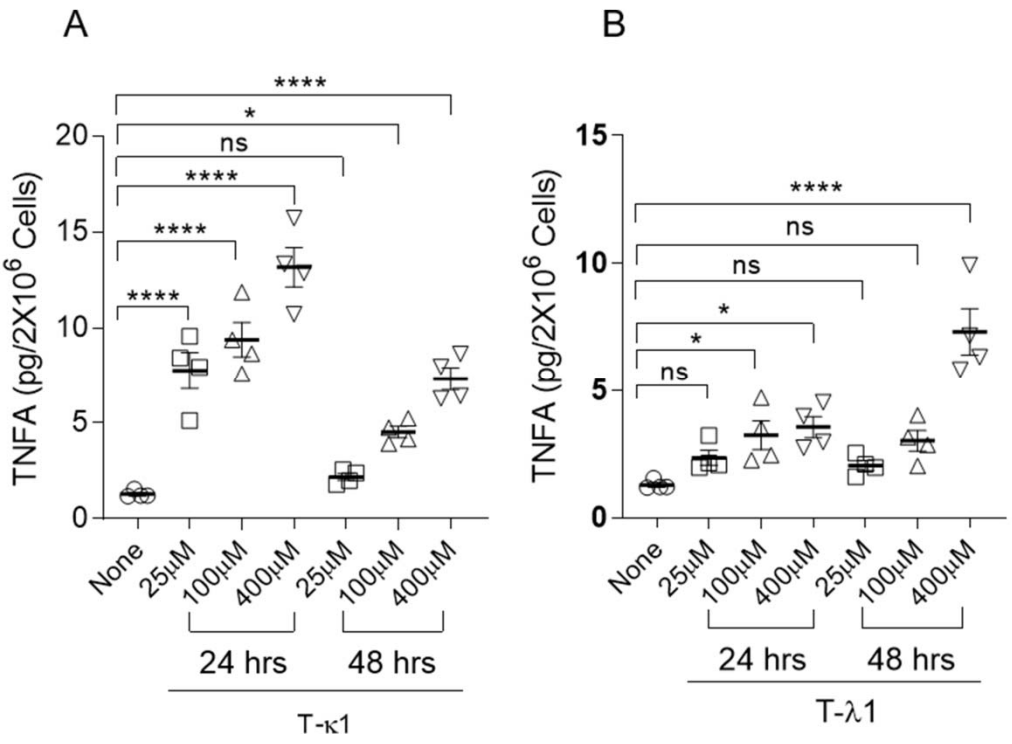

Figure 3. PTCs (RPTECs) incubated with FLCs T-κ1 (A) and T-λ1 (B) increased secretion of TNFA (P<0.05; N=4) in a dose and time dependent manner. *P<0.05, ****P<0.0001; (one-way ANOVA followed by Tukey's multiple comparisons test).

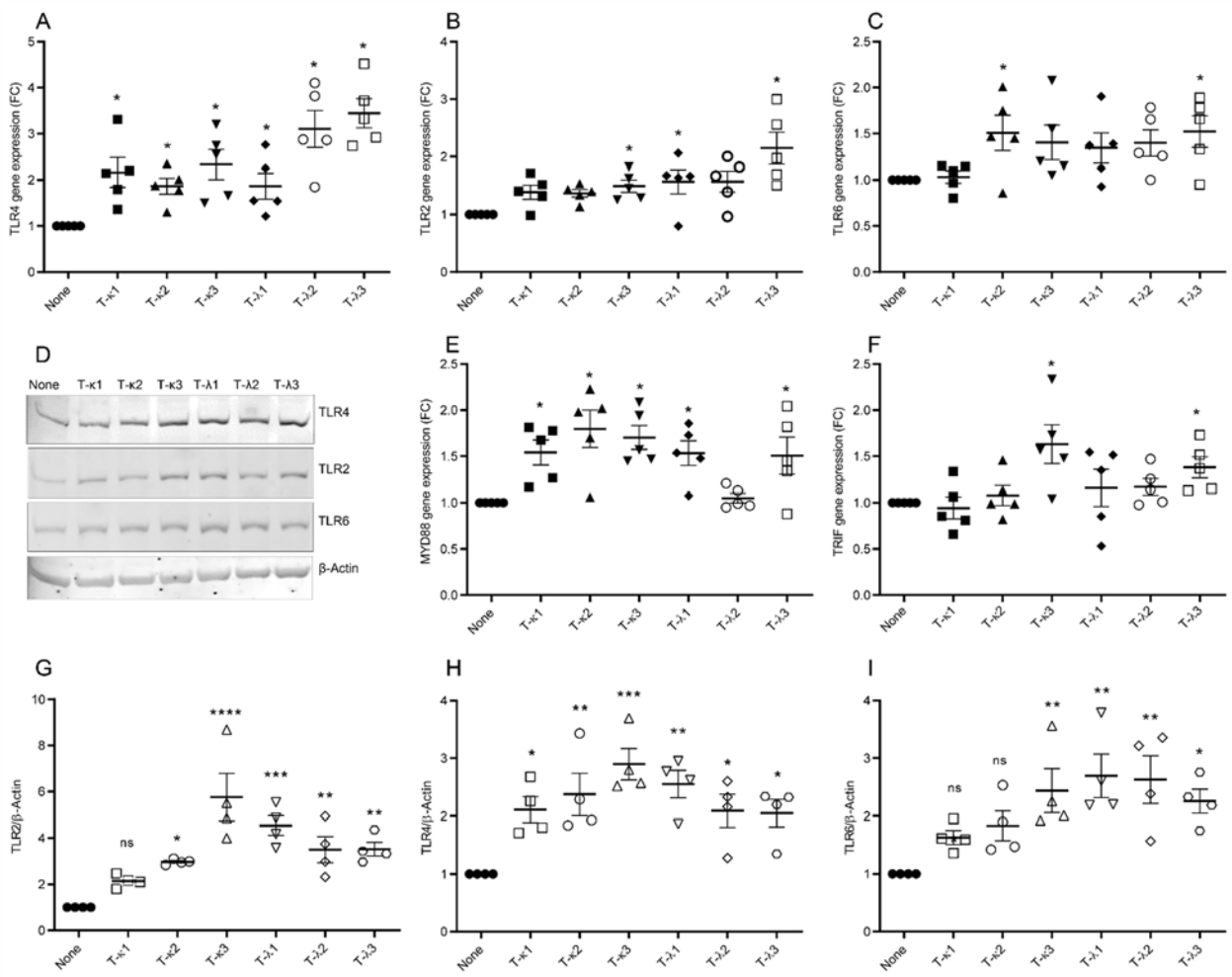

Figure 4. FLCs significantly upregulated gene/protein expression of TLRs 2, 4 and 6 (A-D, G-I) and their adaptor protein molecules MYD88 (E) and TRIF (F) (*P<0.05; N=5) in PTCs (RPTECs). *P<0.05, **P<0.01, ***P<0.001, ****P<0.0001; (one-way ANOVA followed by Tukey's multiple comparisons test).

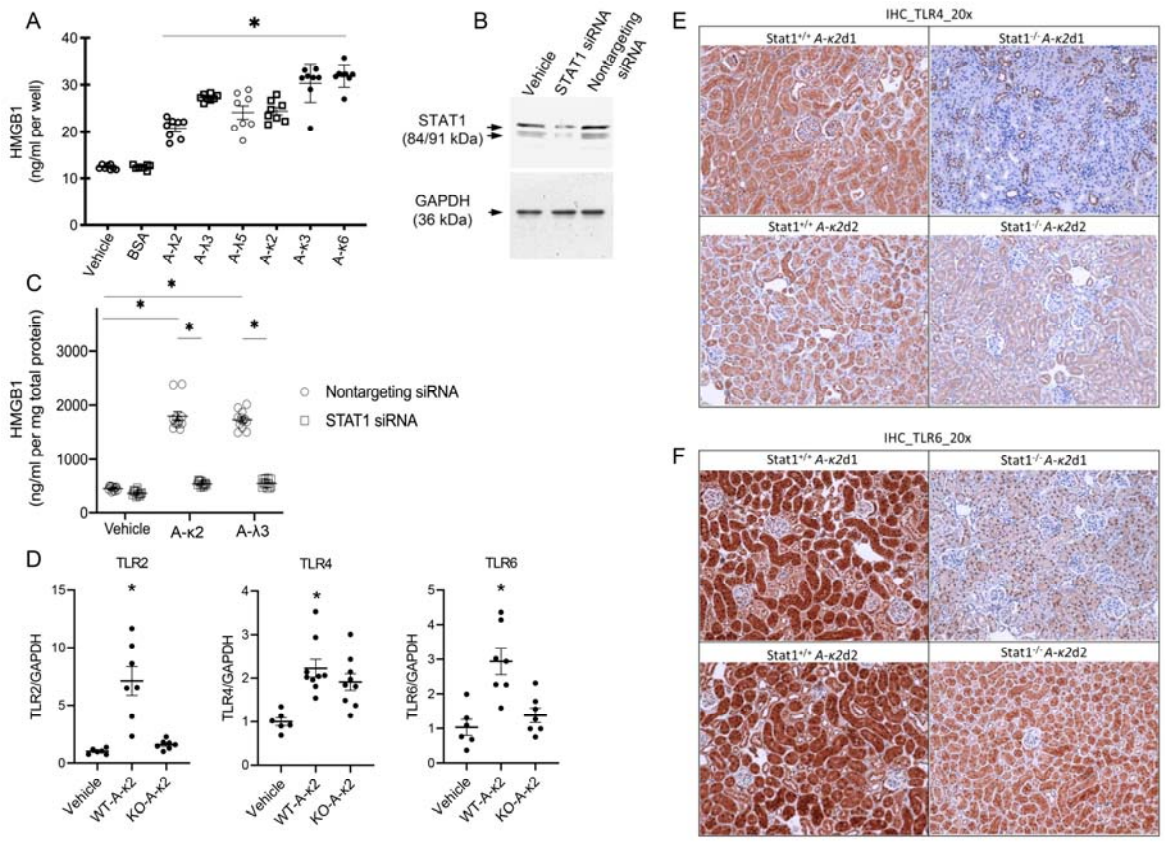

Figure 5. A: Six different FLCs (n=8 samples in each group) increased the release of HMGB1, compared to vehicle-treated and cells incubated in medium containing bovine serum albumin (BSA), 5 mg/ml (*P < 0.0001). Data analyzed using one-way ANOVA; **B**: Treatment with siRNA reduced STAT1 protein levels by about 70-75%; no effect of the nontargeting siRNA on STAT1 was observed; **C**: Knockdown of STAT1 inhibited FLC-induced increases in HMGB1 (n=12 samples in each group) by HK-2 cells. Concentration of HMGB1 in medium divided by total protein of cellular lysates in each sample. Data were analyzed using two-way ANOVA. The analysis comparing the main effects of the FLC and the interaction effect between the FLC and siRNA on HMGB1 showed the main effect for FLC yielded an F ratio of F (2, 66) = 228.1, P < 0.0001, and the effect of siRNA yielded an F ratio of F(1, 66) = 654.3, P < 0.0001. The interaction effect was significant (F ratio of F (2, 66) = 133.2, P < 0.0001). *P < 0.0001;**D**: FLCs induced TLRs 2, 4 and 6 gene expression significantly in WT mice but not in *Stat1*$^{-/-}$ mice; **E-F**: Immunohistochemistry: Representative slides from WT and *Stat1*$^{-/-}$ mice. The WT mice treated with FLCs show positive staining for TLR 4(5E-left panel) and TLR 6 (5F-left panel), *Stat1*$^{-/-}$ kidneys were negative or weakly positive (5E and 5F-left panels). A-κ2- d1 and d2 denote different doses of FLCs injected to mice. Lower dose (termed κ2-d1= 0.033 mg/g BW) or higher dose (termed κ2-d2= 0.165 mg/g BW) of κ2 FLC in PBS. Untreated controls were negative.

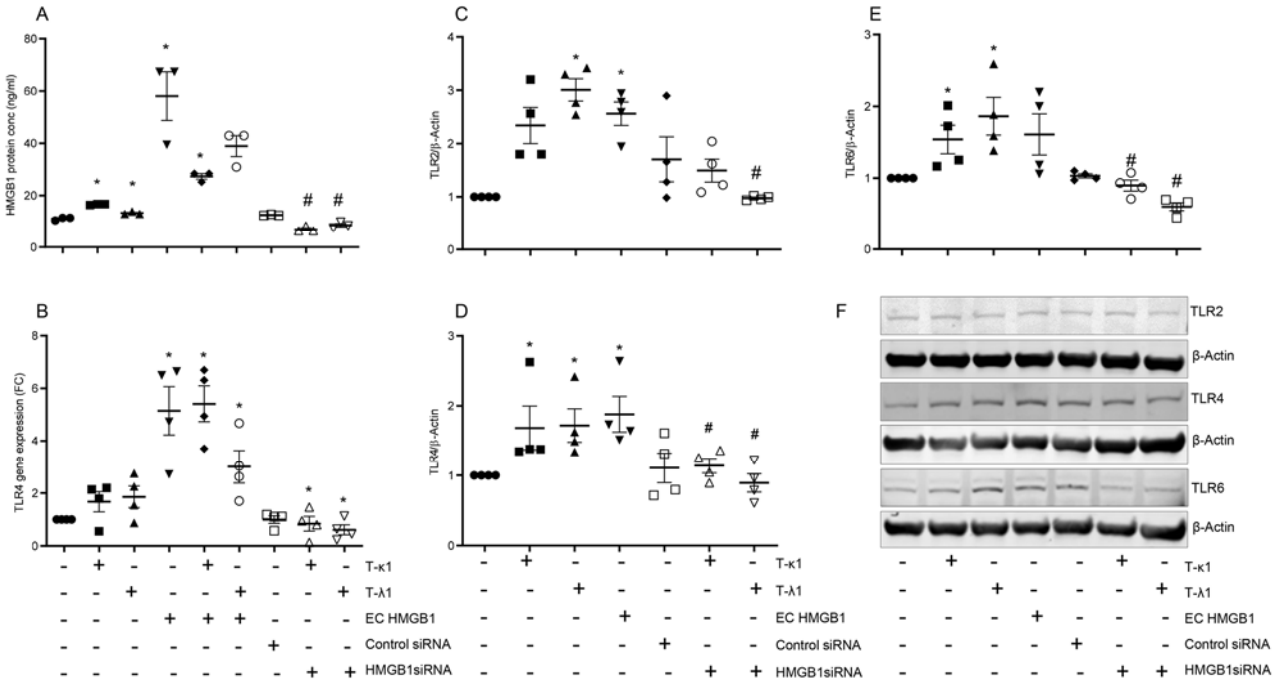

Figure 6. Release of HMGB1 into the medium from cells (RPTECs) exposed to the FLCs and HMGB1 modulators (A); Effect of HMGB1 modulation on the expression of TLR2, TLR4 and TLR6 proteins (B-F); Extracellular HMGB1 used as HMGB1 mimic and HMGB1 siRNA was used as an inhibitor . **P*<0.05; $^{\#}$*P*<0.05; *Compared with No LC; $^{\#}$Compared with FLC (k or λ) (one-way ANOVA followed by Tukey's multiple comparisons test).

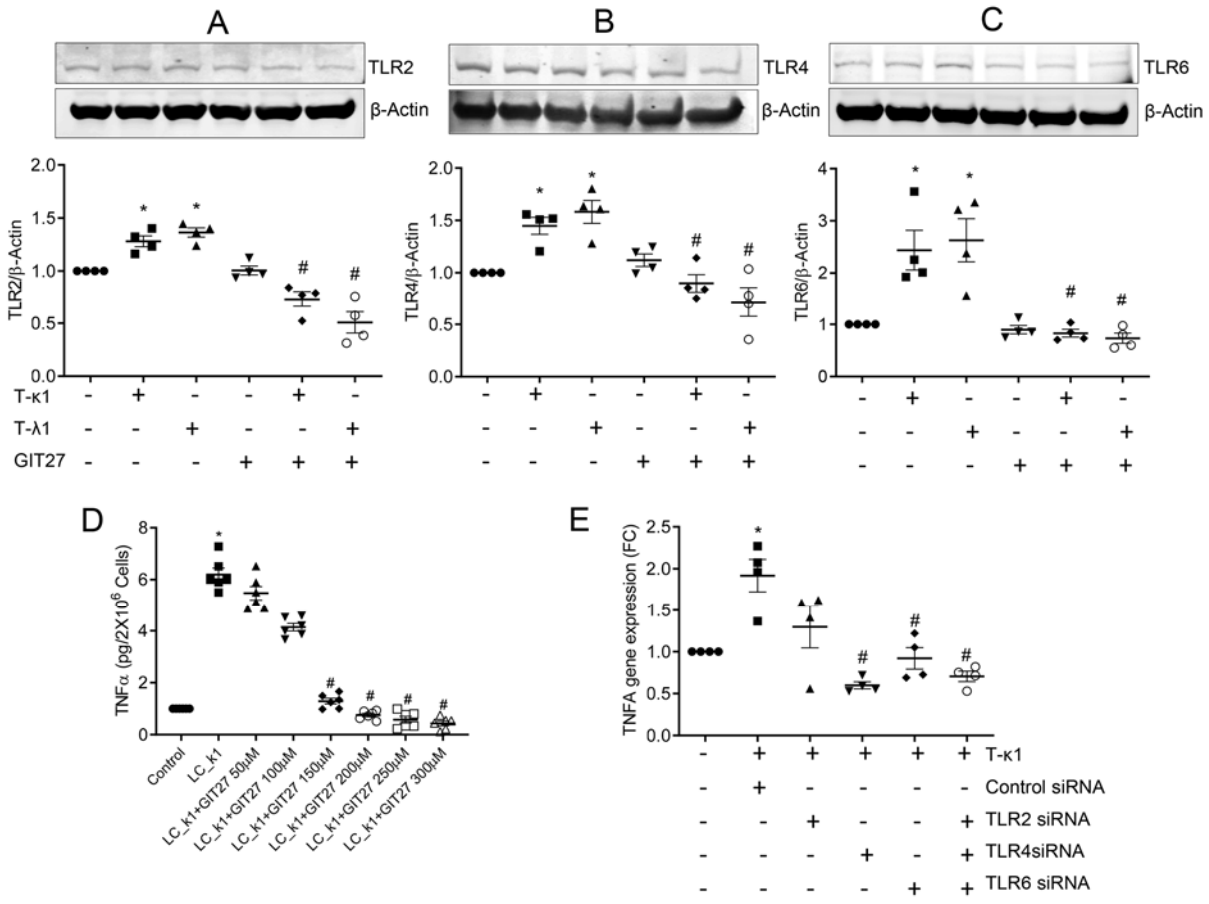

Figure 7. Effect of TLR inhibitor 4,5-Dihydro-3-phenyl-5-isoxazoleacetic acid (GIT27) (A-D) and pooled TLR2/4/6-siRNA (E) on TNFA release by PTCs (RPTECs). N=4; **P*<0.05; $^{\#}$*P*<0.05; *Compared with No LC; $^{\#}$Compared with FLC (k or λ) (one-way ANOVA followed by Tukey's multiple comparisons test).

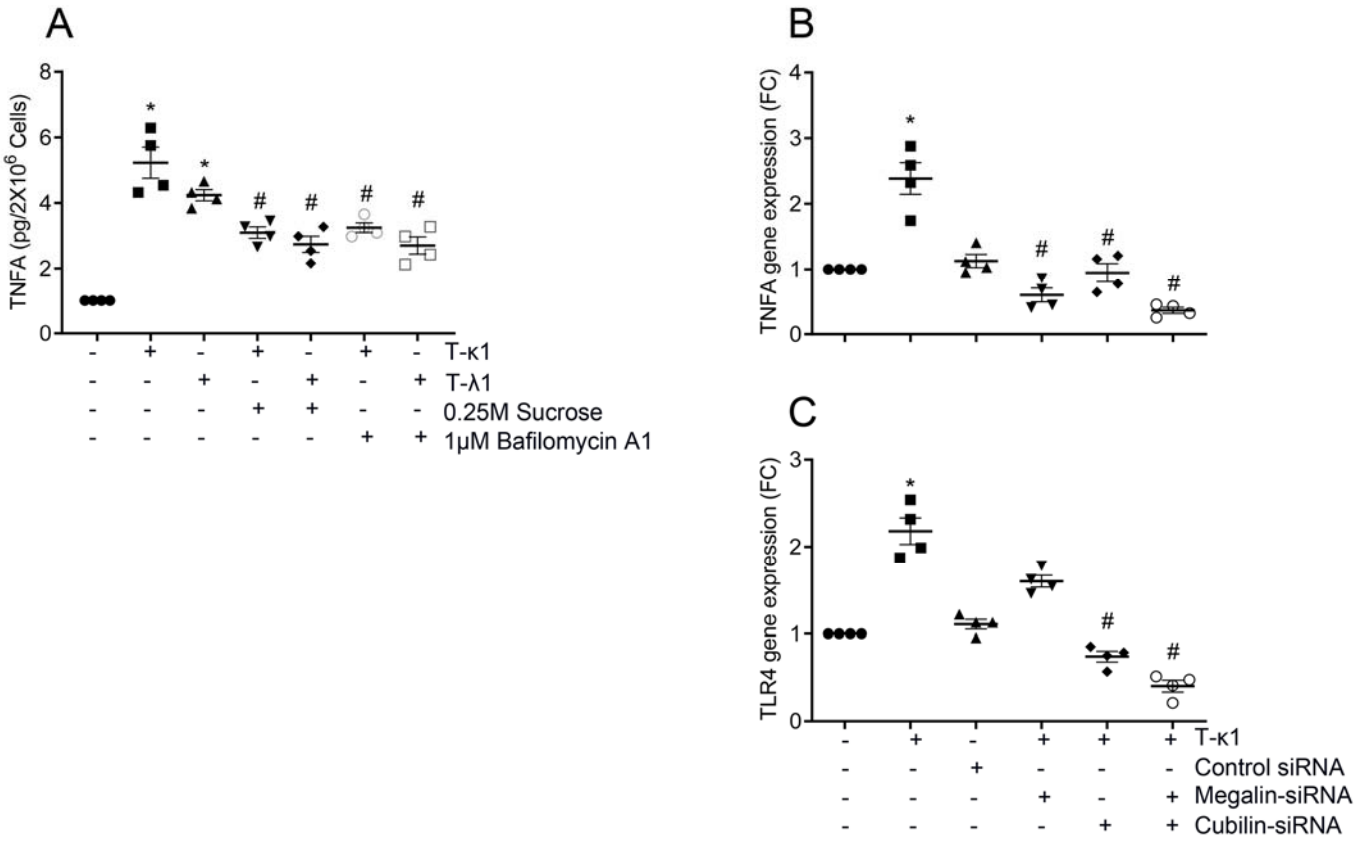

Figure 8. Blocking endocytosis with hypertonic sucrose (0.25M), Bafilomycin A1 (1μM) or Cubilin/ megalin-siRNA ameliorates FLC-induced TNFA release (A-B) in PTCs (RPTECs); Cubilin-Megalin-siRNA synergistically lower the FLC-induced TLR-4 expression (C) in PTCs (RPTECs). N=4; **P*<0.05; #*P*<0.05; *Compared with No LC; #Compared with FLC (k or λ) (one-way ANOVA followed by Tukey's multiple comparisons test).

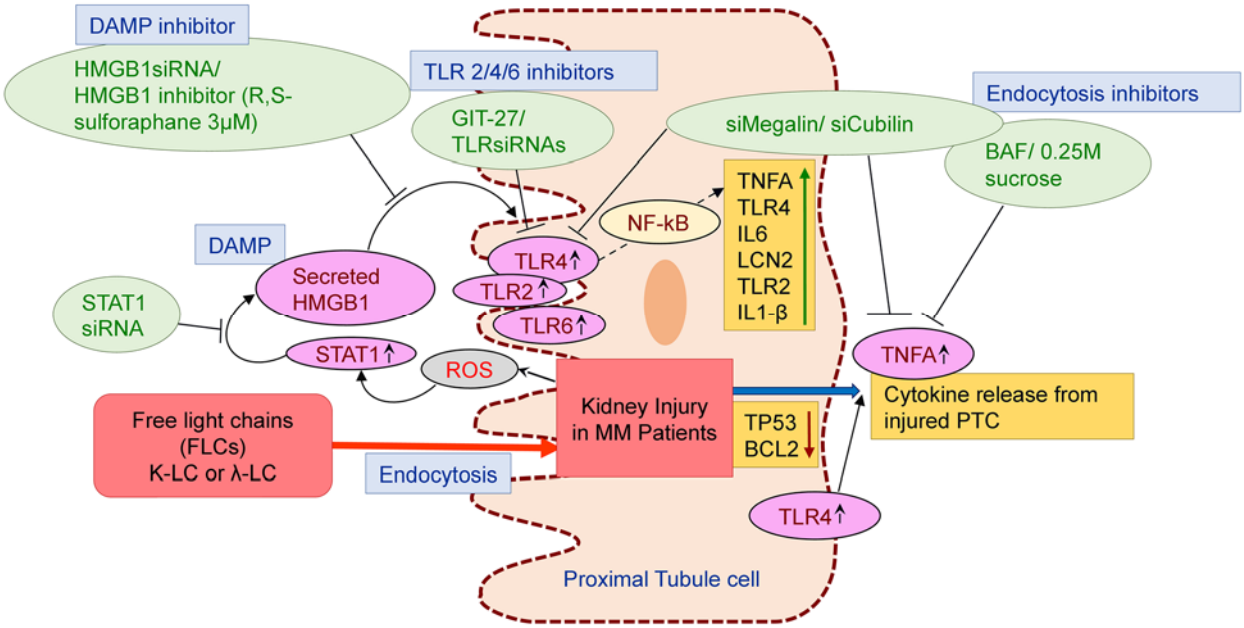

Graphical Abstract.